23rd ABCM International Congress of Mechanical Engineering
December 6-11, 2015, Rio de Janeiro, RJ, Brazil

HORIZONTAL GAS-SOLID PNEUMATIC TRANSPORT: THE EFFECT OF HYDRODYNAMICS USING COMPUTATIONAL FLUID DYNAMICS

Alexandre Marconi de Souza da Costa
Universidade Estadual de Maringá
amscosta@uem.br

Flávio Clareth Colman
Universidade Estadual de Maringá
fccolman@uem.br

Marcelo José Alba
Universidade Tecnológica Federal do Paraná / Universidade Estadual de Maringá
marceloalba@utfpr.edu.br

Paulo Roberto Paraíso
Universidade Estadual de Maringá
paulo@deq.uem.br

Luiz Mário de Matos Jorge
Universidade Estadual de Maringá
lmmj@deq.uem.br

Abstract. *In this work we investigate numerically the pneumatic transport in a horizontal tube. Our modelling is implemented using the open-source code MFIX. For the code, the gas and solid phases are treated as inter-penetrating continua in an Eulerian framework Then, the locally-averaged (continuum) mass, momentum and energy balance, are solved using a modified version of the SIMPLE method. Here, we explore the effect of different parameters from hydrodynamics on the pneumatic transport results: drag relationship between the two phases, method of solution for the solids granular energy, solids stress models, gas-phase turbulence, collisional and frictional coefficients. Towards validation of our modelling, the results are compared with a set of pneumatic transport experimental correlation data from the literature. The degree of accordance points to the better hydrodynamic model to be used.*

Keywords: *pneumatic transport, computational fluid dynamics, MFIX*

1. INTRODUCTION

Pneumatic conveying has increasingly been used in industries to transport bulk materials from one place to another. Proper knowledge of gas and solid flow behaviors can bring significant benefits to energy efficiency, product quality, and pipeline stability. Various theoretical and experimental efforts have been made to study the behaviors of gas and particles for dilute-phase pneumatic conveying, leading to different theoretical and semi-theoretical correlations for the calculation of pressure drop. Recently, the approach of computational fluid dynamics (CFD) has been widely accepted as an effective tool to study pneumatic conveying and other particle–fluid systems (Tsuji, 2007; Zhu *et al.*, 2007, 2008; Van Der Hoef *et al.*, 2008). Different CFD models have been developed and used to study various aspects in pneumatic conveying, as recently discussed by Kuang *et al*. (2008, 2009, 2011). One of the commonly used approaches in CFD to pneumatic conveying modeling is the Eulerian/Eulerian method, with two-fluid continuum models to represent the gas and solid phases as two interpenetrating continua.

In horizontal pneumatic transport of granular solids, the flow features are very complicated because of the action of gravitational forces perpendicular to the flow direction (Owen, 1969). The solids distribution over the cross section of the conveying pipe is substantially influenced by gravitational forces, gas-phase turbulence, collision between particles, and collision between particles and the wall (Huber and Sommer-feld, 1994; Lun and Liu, 1997; Tsuji and Morikawa, 1982) when particles are transported in a horizontal tube by a turbulent gas stream.

In face of the previous shortcomings, the ability to predict the flow behaviors of both gas and solid phases during a typical pneumatic conveying operation or the modes in which the transportation would take place remains limited. Using recently featured characteristics of a state of art CFD code in the area (MFIX- Multiphase Flow with Interphase eXchanges), this paper presents a two-dimensional numerical study of horizontal pneumatic conveyer operating in the dilute region.

2. FUNDAMENTALS

The mathematical model is based on the assumption that the phases can be mathematically described as interpenetrating continua; the point variables are averaged over a region that is large compared with the particle spacing but much smaller than the flow domain (see Anderson, 1967). A short summary of the equations solved by the numerical code in this study are presented next. Refer to Pannala, *et al.*, (2011), Benyahia *et al.* (2006) and Syamlal *et al.* (1993) for more detailment.

The continuity equations for the fluid and solid phase are given by:

$$\frac{\partial}{\partial t}\left(\varepsilon_f \rho_f\right) + \nabla \bullet \left(\varepsilon_f \rho_f \vec{v}_f\right) = 0 \tag{1}$$

$$\frac{\partial}{\partial t}\left(\varepsilon_s \rho_s\right) + \nabla \bullet \left(\varepsilon_s \rho_s \vec{v}_s\right) = 0 \tag{2}$$

In the previous equations ε_f, ε_s, ρ_f, ρ_s, $\vec{v}_f$ and $\vec{v}_s$ are the volumetric fraction, density and velocity field for the fluid and solids phases.

The momentum equations for the fluid and solid phases are given by:

$$\frac{\partial}{\partial t}\left(\varepsilon_f \rho_f \vec{v}_f\right) + \nabla \bullet \left(\varepsilon_f \rho_f \vec{v}_f \vec{v}_f\right) = \nabla \bullet \overline{\overline{S}}_f + \varepsilon_f \rho_f \vec{g} - \vec{I}_{fs} \tag{3}$$

$$\frac{\partial}{\partial t}\left(\varepsilon_s \rho_s \vec{v}_s\right) + \nabla \bullet \left(\varepsilon_s \rho_s \vec{v}_s \vec{v}_s\right) = \nabla \bullet \overline{\overline{S}}_s + \varepsilon_s \rho_s \vec{g} + \vec{I}_{fs} \tag{4}$$

$\overline{\overline{S}}_f$ $\overline{\overline{S}}_s$ are the stress tensors for the fluid and solid phase. It is assumed Newtonian behavior for the fluid and solid phases, i.e.,

$$\overline{\overline{S}} = \left(-P + \lambda\, \nabla \bullet \vec{v}\right)\overline{\overline{I}} + 2\mu\, S_{ij} \equiv -p\,\overline{\overline{I}} + \overline{\overline{\tau}} \qquad S_{ij} = \frac{1}{2}\left[\nabla \vec{v} + \left(\nabla \vec{v}\right)^T\right] - \frac{1}{3}\nabla \bullet \vec{v} \tag{5}$$

In the above equation *P*, λ, μ are the pressure, bulk and dynamic viscosity, respectively.

In addition, the solid phase behavior is divided between a plastic regime (also named as slow shearing frictional regime) and a viscous regime (also named as rapidly shearing regime). The constitutive relations for the plastic regime are related to the soil mechanics theory. Here they are represented as:

$$p_s^p = f_1\left(\varepsilon^*, \varepsilon_f\right) \qquad \mu_s^p = f_2\left(\varepsilon^*, \varepsilon_f, \phi\right) \tag{6}$$

In the above equation ε^* is the packed bed void fraction and ϕ is the angle of internal friction. A detailing of functions f_1 to f_9 can be obtained in Benyahia (2008). On the other hand, the viscous regime behavior for the solid phase is ruled by two gas kinetic theory related parameters (e, Θ).

$$p_s^v = f_3\left(\varepsilon_s, \rho_s, d_p, \Theta, e\right) \qquad \mu_s^v = f_4\left(\varepsilon_s, \rho_s, d_p, \Theta^{1/2}, e\right) \tag{7}$$

The solid stress model outlined by Eqs. (6) and (7) will be quoted here as the standard model. In the MFIX code, for monodisperse system of particles in the viscous regime, different correlations following the works of Cao and Ahmadi (1995), Iddir & Arastoopour (2005), Lun *et al* (1984), Simonin (1996) are available. Additionally, a general formulation for the solids phase stress tensor that admits a transition between the two regimes is given by*:*

$$\overline{\overline{S}}_s = \begin{cases} \phi\left(\varepsilon_f\right)\overline{\overline{S}}_s^v + \left[1 - \phi\left(\varepsilon_f\right)\right]\overline{\overline{S}}_s^p & \text{if } \varepsilon_f < \varepsilon^* + \delta \\ \overline{\overline{S}}_s^v & \text{if } \varepsilon_f \geq \varepsilon^* + \delta \end{cases} \tag{8}$$

According to Pannala *et al.*(2009), two different formulations for the weighting parameter "ϕ" can be employed:

$$\phi(\varepsilon)=\frac{1}{1+\upsilon^{\frac{\varepsilon-\varepsilon^*}{2\delta\varepsilon^*}}}\Rightarrow\phi(\varepsilon)=\frac{\mathrm{Tanh}\left(\frac{\pi\left(\varepsilon-\varepsilon^*\right)}{\delta\varepsilon^*}\right)+1}{2} \tag{9}$$

In the above equation the void fraction range δ and the shape factor υ are smaller values less than unity. It must be emphasized that when δ goes to zero and ϕ equals to unity, the "switch" model as proposed by Syamlal *et al.* (1993) based on the Schaeffer (1987) can be recovered.

On the other hand, the Srivastava and Sundaresan (2003), also called "Princeton model", can be placed on the basis of Eq. (9)

Also in equations (4) and (5) $\vec{\mathrm{I}}_{\mathrm{fs}}$ is the momentum interaction term between the solid and fluid phases, given by

$$\vec{\mathrm{I}}_{\mathrm{fs}}=-\varepsilon_s\nabla P_f-\beta\left(\vec{v}_s-\vec{v}_f\right) \tag{10}$$

There is a number of correlations for the drag coefficient β (Eqs. 11 to 16). The first of the correlations for the drag coefficient is based on Wen and Yu (1966) work. The Gidaspow drag coefficient is a combination between the Wen Yu correlation and the correlation from Ergun (1952). The Gidaspow blended drag correlation allows controlling the transition from the Wen and Yu, and Ergun based correlations. In this correlation the χ blending function was originally proposed by Lathowers and Bellan (2000) and the value of parameter *C* controls the degree of transition. From Eq. (14), the correlation proposed by Syamlal and O'Brien (1993) carries the advantage of adjustable parameters C_1 and d_1 for different minimum fluidization conditions. The correlations given in Eq. (15) and Eq. (16) are based on Lattice-Boltzmann simulations. For detailments of these last drag correlations refer to the works by Benyahia *et al.* (2006) and Wang *et al.* (2010).

$$\beta_{\text{Wen-Yu}}=\frac{3}{4}C_D\frac{\rho_f\varepsilon_f\varepsilon_s\left|\vec{v}_f-\vec{v}_s\right|}{d_p}\varepsilon_f^{-2.65}\qquad C_D=\begin{cases}\dfrac{24}{\mathrm{Re}}\left(1+0.15\,\mathrm{Re}^{0.687}\right) & \mathrm{Re}<1000\\ 0.44 & \mathrm{Re}\geq 1000\end{cases}\qquad \mathrm{Re}=\frac{\rho_f\varepsilon_f\left|\vec{v}_f-\vec{v}_s\right|d_p}{\mu_f} \tag{11}$$

$$\beta_{\text{Gidaspow}}=\begin{cases}\beta_{\text{Wen-Yu}} & \varepsilon_f>0.8\\ \beta_{\text{Ergun}}=\dfrac{150\,\varepsilon_s\left(1-\varepsilon_s\right)\mu_f}{\varepsilon_f d_p^2}+\dfrac{1.75\,\rho_f\varepsilon_s\left|\vec{v}_f-\vec{v}_s\right|}{d_p} & \varepsilon_f\leq 0.8\end{cases} \tag{12}$$

$$\beta_{\text{Gidaspow-blended}}=\chi\,\beta_{\text{Wen-Yu}}+(1-\chi)\beta_{\text{Ergun}}\qquad \chi=\frac{\tan^{-1}\left(C\,\left(\varepsilon_f-0.8\right)\right)}{\pi}+0.5 \tag{13}$$

$$\begin{gathered}\beta_{\text{Syamlal-OBrien}}=\frac{3}{4}\frac{\rho_f\varepsilon_f\varepsilon_s}{V_r^2 d_p}\left(0.63+4.8\sqrt{\frac{V_r}{\mathrm{Re}}}\right)^2\left|\vec{v}_f-\vec{v}_s\right|\\ V_r=0.5A-0.03\,\mathrm{Re}+0.5\times\sqrt{\left(0.06\,\mathrm{Re}\right)^2+0.12\,\mathrm{Re}\,\left(2B-A\right)+A^2}\\ A=\varepsilon_f^{4.14}\quad B=\begin{cases}C_1\varepsilon_f^{1.28} & \varepsilon_f\leq 0.85\\ \varepsilon_f^{d_1} & \varepsilon_f>0.85\end{cases}\end{gathered} \tag{14}$$

$$\beta_{\text{Koch-Hill}}=18\mu_f\left(1-\varepsilon_s\right)^2\varepsilon_s\frac{F}{d_p^2}\qquad F=f_9\left(F_0,F_1,F_2,F_3\right) \tag{15}$$

$$\beta_{BVK} = 180\frac{\mu_f \varepsilon_s^2}{d_p^2} + 18\frac{\mu_f \varepsilon_f^3 \varepsilon_s \left(1+1.5\sqrt{\varepsilon_s}\right)}{d_p^2} + 0.31\frac{\mu_f \varepsilon_s \,\mathrm{Re}}{\varepsilon_f d_p^2}\frac{\left[\varepsilon_f^{-1} + 3\varepsilon_f\varepsilon_s + 8.4\,\mathrm{Re}^{-0.343}\right]}{\left[1+10^{3\varepsilon_s}\,\mathrm{Re}^{-0.5-2\varepsilon_s}\right]} \tag{16}$$

For closing the model, a transport equation for the granular energy Θ provides a way of determine the pressure and viscosity for the solid phase during the viscous regime. Equation (5) is a transport equation for the granular energy Θ. Its solution provides a way of determine the pressure and viscosity for the solid phase during the viscous regime. The terms κ_s γ and ϕ_{gs} are the granular energy conductivity, dissipation and exchange, respectively.

$$\frac{3}{2}\left[\frac{\partial}{\partial t}\varepsilon_s\rho_s\Theta + \nabla\bullet\rho_s\vec{v}_s\Theta\right] = \overline{\overline{S}}_s : \nabla\vec{v}_s - \nabla\bullet\left(\kappa_s\nabla\Theta\right) - \gamma + \phi_{gs} \tag{17}$$

$$\kappa_s = f_5\left(\varepsilon_s, \rho_s, d_p, \Theta^{1/2}, e, \beta\right) \qquad \gamma = f_6\left(\varepsilon_s, \rho_s, d_p, \Theta^{3/2}, e\right) \qquad \phi_{gs} = f_7\left(\varepsilon_s, \rho_s, d_p, \Theta, \left|\vec{v}_f - \vec{v}_s\right|, \beta\right) \tag{18}$$

In the algebraic approach, instead solving the full equation (6), the granular energy is obtained by equating the first term on the right hand side with the dissipation term.

The models where equations in the form of Eqs (5) to (8) and (17) are solved are kinetic theory models. In the MFIX code there is number of kinetic models implemented: IA_NONEP (Iddir and Arastoopour, 2005), LUN_1984 (Lun *et al.*, 1984), AHMADI (Cao and Ahmadi, 1995), SIMONIN (Simonin, 1996).

Following the approach of Benyahia *et al* (2007) for dilute systems, in this study is compared the influence of three wall boundary condition (BC) for the particulate solids: Johnson and Jackson, Jenkins, and free slips for solids with a specified granular energy of zero at wall. The Johnson and Jackson wall BC for solids velocity and granular temperature, presented in Eq. (19), uses a specularity coefficient ϕ that describes the roughness of the wall; a value of zero refers to perfectly diffuse collisions. The Jenkins BC, described in Eq. (20), depends on the value of particle-wall restitution coefficient e_w and friction coefficient μ_f^+. For the forms of functions f_8 to f_{11} and values of the parameters described previously, refer to the work of Benyahia *et al.* (2007).

$$\mu_s\frac{\partial u_s}{\partial x} = f_8\left(\phi, \rho_s, \varepsilon_s, \Theta, u_s, g_0, \varepsilon_s^{max}\right) \qquad \kappa_s\frac{\partial\Theta}{\partial x} = f_9\left(\phi, \rho_s, \varepsilon_s, \Theta, u_s, g_0, \varepsilon_s^{max}\right) \tag{19}$$

$$\mu_s\frac{\partial u_s}{\partial x} = f_{10}\left(p_s, \mu_f^+, u_s\right) \qquad \kappa_s\frac{\partial\Theta}{\partial x} = f_{11}\left(p_s, \Theta, \mu_f^+, e_w\right) \tag{20}$$

In this work, the CFD results were compared against the correlation by Konno and Saito (1969), and adapted according to Klinzing *et al.* (2010), as presented in Equations (21) to (24):

$$\frac{\Delta P}{H} = 2\, f_L\frac{\rho_f\left(v^2\right)\varepsilon}{D} + 4\ 0.0285\ \left(g\ D\right)^{1/2}\left(c^{-1}\right)\ \rho_s\ \frac{1-\varepsilon}{2\,D}\ c^2 \tag{21}$$

$$f_L = 0.0014 + 0.125\cdot Re^{-0.32} \qquad Re = \frac{\rho_f\ v\, D}{\mu_f} \tag{22}$$

$$\varepsilon = 1 - \mu^*\cdot\left(\rho_f/\rho_s\right)\cdot\left(v_\varepsilon/c\right) \qquad v_\varepsilon = v/\varepsilon \tag{23}$$

$$\mu^* = \frac{\dot{m}_s}{\left(\pi/4\right)\cdot D^2\cdot\rho_f\cdot v} \qquad c = v\cdot\left(1 - 0.68\, d_p^{\,0.92}\cdot\left(\rho_s\right)^{0.5}\cdot\rho_f^{-0.2}\cdot D^{-0.54}\right) \tag{24}$$

In the previous equations ΔP is the pressure loss in Pa, H is the tube length in m, f_L is the gas friction factor. v and ε are the characteristics gas superficial velocity (m/s) and voidage, respectively. D is the tube diameter (m) and g is the gravity accelerations value (9.81 m/s^2). In Eqs (22) to (24) are presented the corresponding equations for obtaining the remaining terms in Eq. (21). Also, in Eq. (24), $\dot{m}_s$ represents the solids loading, in kg/s.

3. METHODOLOGY

MFIX (Multiphase Flow with Interphase eXchanges) is an open source CFD code developed at the National Energy Technology Laboratory (NETL) for describing the hydrodynamics, heat transfer and chemical reactions in fluid-solids systems. It has been extensively used for describing bubbling and circulating fluidized beds, spouted beds and gasifiers. MFIX calculations give transient data on the three-dimensional distribution of pressure, velocity, temperature, and species mass fractions.

The numerical runs were based on a cylindrical two-dimensional coordinate system as depicted in Fig. 1. The grid employed, obtained after mesh refinement studies, represents a trade off between computational cost, and the degree of accuracy required to compare results with the chosen literature correlation.

In this work, the parameters for controlling the numerical solution (e.g., under-relaxation, sweep direction, linear equation solvers, number of iterations, residual tolerances) were kept as their default values. Also, for setting up the mathematical model, when not otherwise specified the code default values were used.

For generating the numerical results and comparison with experimental results, we employed the parameters given in Table 1, referred here as baseline simulation, correspondent to a typical dilute pneumatic conveying situation. Moreover, for the baseline simulation we employed the Syamlal-O´Brien drag model, the standard solid stress model, and slip and non-slip condition for solid and gas phase, correspondingly. The previous set of models will be referred in the results section as baseline simulation models.

Table 1. Baseline geometry and physical parameters for CFD simulation

H = 10 m	D = 0.1 m
H1 = 0.3 m	$\mu_f = 2.0\ 10^{-5}$ kg/m s
H2 = 0.2 m	$\rho_f = 1.2$ kg/m^3
$\dot{m}_s = 0.28$ kg/s	$d_p = 250$ μm
grid: 10 × 1000	ρ_s =2000 kg/m^3
V = 10, 20, 30 m/s	
Simulation time: 20 s	

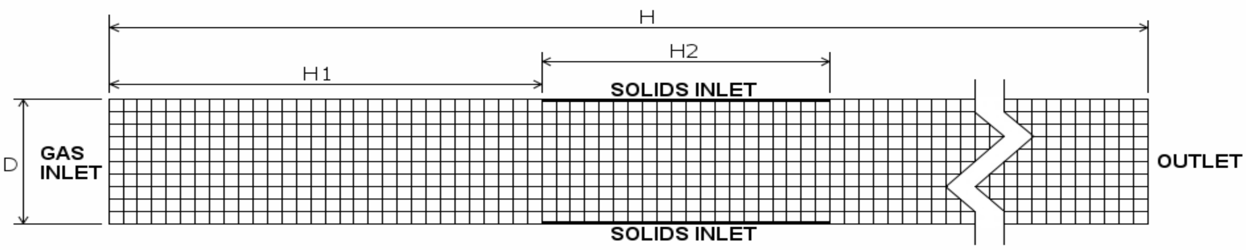

Figure 1. Geometry and mesh for numerical simulation

4. RESULTS AND DISCUSSION

Next, the results from CFD simulations will be presented in terms of friction coefficient f (= $2\Delta PD/\rho_f v^2 H$) and Re (defined in the Eq. 22) corresponding to the three velocities in Table 1 (Re_1 = 64182; Re_2 = 128364; Re_3 = 192547). In Fig. 2 is presented the results corresponding to the influence of the drag correlation. In Fig. 3 is presented the influence of the kinetic theory model for the solids phase stress representation. In Fig. 4 is presented the influence of the wall boundary condition on the results.

Analysis of Fig. 2 shows that the predicted f values are mildly influenced by the drag correlation in the range of Reynolds investigated. Figure also displays around 6% deviation between the values predicted using different drag models for the lowest Reynolds investigated. This behavior is consistent, as expected that for low Reynold's number, corresponding for smaller gas velocities, the effect of interaction between gas-solid is more pronounced, i.e., the system is less diluted.

Analysis of Fig. 3 shows the influence of the kinetic theory model for describing the solids stresses for the particulate phase. As it can be seen, the kinetic theory model significantly influences the predicted f, with 30 % difference between the algebraic and Simonin model. This difference can be explained in terms of similarity of the algebraic model to a zero-equation single-phase turbulence model, and the kinetic models to a one-equation single-phase turbulence model. In this way when the partial differential equation for the granular energy is solved with any of the kinetic theory models is expected the capture of further spatial and temporal details of the flow.

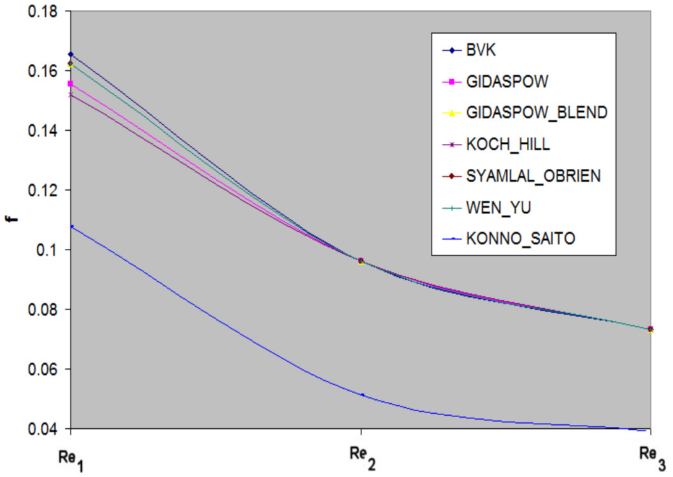

Figure 2. Effect of different drag models

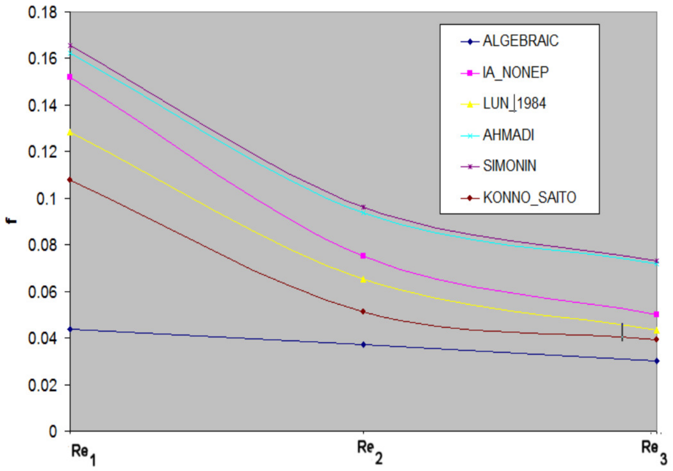

Figure 3. Effect of different solids stress kinetic theory model

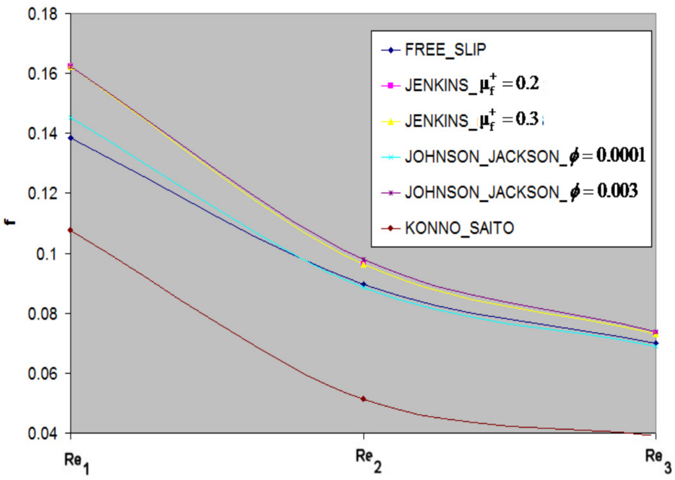

Figure 4. Effect of different solids boundary conditions

From Fig. 4, the type of solids BC in the wall impacts less (20 difference) than the kinetic theory model, although its effect is more significant than the influence of the drag correlations. Similarly to be outlined, from Fig. 2, there is a decrease under the influence for high Reynold's number, as a more dilute flow with gas dominated regime is approached.

Finally, the curves' trends in the Reynolds number are similar to the behavior predicted by Konno-Saito correlation. On the other hand, the predicted values, except those of the algebraic model for solids stresses, are higher than Konno and Saito's correlation. The results suggest that a best agreement can be reached using an appropriate choice of drag correlation, kinetic theory model and solids boundary condition. It must be pointed that this best degree of accordance must be chased inside the domain of the Konno-Saito experimental work, specifically, values below 20 m/s and 0.05 m, for gas velocities and tube diameter, respectively.

5. CONCLUSIONS

In this work was studied with the help of a state of art CFD code, pressure drop aspects of the dilute horizontal transport pneumatic conveying of solids. The results points that the influence of drag correlation is greater for low Reynolds number. The kinetic theory model impacts more the results. The influence of BC, could be accessed, and is higher in a more dilute (low Reynolds number). It must be pointed, a further exploring of the validation procedure along with a experimental rig assembly is in progress.

6. ACKNOWLEDGEMENTS

The authors would like to thank CAPES and Araucária Foundation for financial support and the National Supercomputing Center (CESUP), of the Federal University of Rio Grande do Sul (UFRGS) for the availability of resources and technology for the development of this research.

7. REFERENCES

Anderson, T. B., 1967. A fluid mechanical description of fluidized beds: Equations of motion, *Industrial Engineering Chemical Fundamentals*, Vol 6, pp. 527-539.

Benyahia, S., 2008. Validation study of two continuum granular frictional flow theories, *Industrial Engineering Chemical Research*, Vol. 47, p. 8926-8932.

Benyahia, S., Syamlal, M., O'Brien, T. J., 2007. Study of the Ability of Multiphase Continuum Models to Predict Core-Annulus Flow. *AIChe Journal*, Vol. 53 (10), 2549-2562.

Benyahia, S., Syamlal, M., O'Brien, T. J., 2006. *Summary of MFIX Equations 2005-4*, 1 March 2006: <http://www.mfix.org/documentation/MfixEquations2005-4-1.pdf>.

Benyahia, S., Syamlal, M., O'Brien, T. J., 2006. Extension of Hill–Koch–Ladd drag correlation over all ranges of Reynolds number and solids volume fraction. *Powder Technology*, Vol. 162, p. 166-174.

Cao, J., Ahmadi, G., 1995. Gas-particle two-phase turbulent flow in a vertical duct. *Int. J. Multiphase Flow*, Vol. 21(6), p. 1203-1228.

Ergun, S., 1952. Fluid-flow through packed columns. *Chemical Engineering Progress*, Vol. 48, n. 2, p. 91-94.

Huber, N., and M. Sommerfeld, 1994. Characterization of the Cross-Sectional Particle Concentration Distribution in Pneumatic Conveying Systems. *Powder Technol.*, Vol. 79, p. 191.

Iddir, H., Arastoopour, H., 2005. Modeling of multitype particle flow using the kinetic theory approach, *AIChE J.* Vol. 51(6), p. 1620-1632.

Klinzing, G. E., Rizk, F., Marcus, R., Leung, L.S., 2010. *Pneumatic Conveying of Solids: A Theoretical and Practical Approach*. 3rd ed, Springer.

Konno, H. Saito, S., 1969. Pneumatic conveying of solids through straigh pipes. *Journal of Chemical Engineering Japan*, p. 211-216

Kuang, S.B., Chu, K.W., Yu, A.B., Zou, Z.S., Feng, Y.Q., 2008. Computational investigation of horizontal slug flow in pneumatic conveying. *Ind. Eng. Chem. Res.* Vol. 47, p. 470–480.

Kuang, S.B., Yu, A.B., 2011. Micromechanic modeling and analysis of the flow regimes in horizontal pneumatic conveying. *AIChE J.* Vol. 57, p. 2708–2725.

Kuang, S.B., Yu, A.B., Zou, Z.S., 2009. Computational study of flow regimes in vertical pneumatic conveying. *Ind. Eng. Chem. Res.* Vol. 48, p. 6846–6858.

Lathowers, D., Bellan, J., 2000. Modeling of dense gas-solid reactive mixtures applied to biomass pyrolysis in a fluidized bed. *Proceedings of the 2000 U.S. DOE Hydrogen Program Review*, NREL/CP-570-28890. USA.

Lun, C. K. K., and H. S. Liu, 1997. Numerical Simulation of Dilute Turbulent Gas-Solid Flows in Horizontal Channels. *Int. J. Multiphase Flow*, 23, p. 575.

Lun, C. K. K., Savage, S. B., Jeffrey, D. J., Chepurniy, N., 1984. Kinetic Theories for granular flow: inelastic particles in couette flow and slightly inelastic particles in a general flow, *J. Fluid Mech.*, Vol. 140, p. 223-256.

Owen, P. R., 1969. Pneumatic Transport. *J. Fluid Mech.*, Vol. 39, p. 407.

Pannala, S., Daw, C. S., Finney, C. E. A., Benyahia, S., Syamlal, M., O´Brien, T. J., 2009. Modelling the collisional-plastic stress transition for bin discharge of granular material. *Powders and Grains – Proceeding of the 6th International Conference on Micromechanics of Granular Media*, p. 657-660.

Pannala, S., Syamlal, M., O'Brien, T., 2011. *Computational Gas-Solids Flows and Reacting Systems: Theory, Methods and Practice, Engineering Science Reference*. Hershey, New York.

Schaeffer, D. G., 1987. Instability in the evolution equations describing incompressible granular flow", *Journal Differential Equations*, Vol. 66, p. 19-50.

Simonin, 1996. VKI Lecture Series, 1996-2

Siravastava, A., Sundaresan, S., 2003. Analysis of a frictional–kinetic model for gas–particle flow. *Powder Technology*, Vol. 129, p. 72-85.

Syamlal, M., Rogers, W. A., O'Brien, T. J., 1993. *MFIX Documentation, Theory Guide. Technical Note*, DOE/METC-94/1004, NTIS/DE94000087, National Technical Information Service, Springfield, VA, USA.

Tsuji, Y., 2007. Multi-scale modeling of dense phase gas–particle flow. *Chem. Eng. Sci*. Vol. 62, p. 3410–3418.

Tsuji, Y., and Y. Morikawa, 1982. LDV Measurements of Air-Solid Two-Phase Flow in a Horizontal Pipe. *J. Fluid Mech*., Vol. 120, p. 385.

Van Der Hoef, M.A., Annaland, M.V., Deen, N.G., Kuipers, M., 2008. Numerical simulation of dense gas–solid fluidized beds: a multiscale modeling strategy. *Annu. Rev. Fluid Mech*. Vol. 40, p. 47–70.

Wang, J., van der Hoef, M. A., Kuipers, J. A. M., 2010. CFD study of the minimum bubbling velocity of Geldart A particles in gas-fluidized beds, *Chemical Engineering Science*, Vol. 65, p. 3772-3785.

Wen, C. Y., Yu, Y. H., 1966. Mechanics of Fluidization. *Chemical Engineering Progress Symposium Series*, Vol 62, p. 100-111.

Zhu, H.P., Zhou, Z.Y., Yang, R.Y., Yu, A.B., 2007. Discrete particle simulation of particulate systems: theoretical developments. *Chem. Eng. Sci.* Vol. 62, p. 3378–3396.

Zhu, H.P., Zhou, Z.Y., Yang, R.Y., Yu, A.B., 2008. Discrete particle simulation of particulate systems: a review of mayor applications and findings. *Chem. Eng. Sci*. Vol. 63, p. 5728–5770.

8. RESPONSIBILITY NOTICE

The authors are the only responsible for the printed material included in this paper.